Evaluation of Solar Energy Losses for the Heliostat-to-Receiver Path of a Tower Solar Plant for Different Aerosol Models

Gabriel López[1], Christian A. Gueymard[2] and Juan Luis Bosch[1]

[1] Dpto. Ingeniería Eléctrica y Térmica, de Diseño y Proyectos, Universidad de Huelva, Huelva (Spain)

[2] Solar Consulting Services, Colebrook, NH (USA)

Abstract

The efficiency of solar tower plants is impacted twice by atmospheric aerosols. First, aerosols attenuate the direct solar irradiance reaching the heliostats, and then reduce the irradiance reflected by these heliostats while it propagates to the receiver. The aerosol transmittance from the top of atmosphere to the ground is well modeled by many radiative transfer codes, but its counterpart for the heliostat-to-receiver slant path has only been estimated for a very limited number of ideal atmospheric conditions. In this work, the solar losses for the heliostat-to-receiver slant paths are extensively analyzed for different aerosol models, atmospheric conditions, and mirror-to-tower geometries by performing detailed simulations with the MODTRAN radiative transfer code. Reductions up to 30% of the solar irradiance incident on distant heliostats can occur under moderately turbid situations, due to the concentration of aerosols near the ground. It is found that site elevation is not a significant factor, contrary to what was anticipated, according to an old empirical model of the literature.

Keywords: Solar tower plants, transmission losses, aerosol models, atmospheric attenuation, CSP.

1. Introduction

The accurate evaluation of the irradiance reaching the receiver of a Tower Solar Power plant (TSP) is of primary importance to prepare its design, and later evaluate its actual performance. The literature mentions numerous radiative transfer models (e.g., SMARTS, libRadtran, or MODTRAN) that can derive the spectral aerosol transmittance from the top of the atmosphere to the surface with sufficient accuracy for normal plant operation, provided that the bulk aerosol optical properties are known over the vertical column. Most of these models, however, are not suitable to easily predict the atmospheric radiation losses over the heliostat-to-receiver slant path. Such calculations are complex, time consuming, and require specific inputs (such as vertical aerosol profiles) that are usually not known. Moreover, most models (with the notable exception of MODTRAN, or its predecessor, LOWTRAN) are not designed to calculate the radiation transmission over short slant paths in any arbitrary direction. Some efforts were conducted several decades ago to derive simple empirical parameterizations from detailed modeling and obtain such results in a more accessible form. Examples include the empirical Pitman and Vant-Hull model (1981), as well as modules that are part of the DELSOL and MIRVAL CSP design codes, for instance. The main drawback of this approach is the extremely limited number of possible atmospheric conditions, i.e., lack of general validity. In this respect, the range of possible atmospheric conditions that these simplified models can handle is limited to a few visibility values only (typically 23 km and 5 km). Originally, such values were assumed to describe clear conditions and hazy conditions, respectively.

In recent years, this topic has gathered renewed interest, so that new studies have been conducted to improve this type of algorithm (Gueymard et al., 2017; Hanrieder et al., 2016, 2017; Sengupta and Wagner, 2012). Previous investigations by the authors have shown that the attenuation specifically caused by water vapor near the surface was significant, albeit small in comparison to that of aerosols (Gueymard et al., 2017; López et al., 2016). In addition, the measurement of horizontal visibility for the specific needs of the TSP industrial sector has progressed, with the development of several low-cost automatic devices, such as forward-scatter-based visibilimeters (Hanrieder et al., 2017). Some of the first studies using the latter technology report that visibility

doi:10.18086/swc.2017.23.03 Available at http://proceedings.ises.org

values are commonly much higher than 23 km (López et al., 2017). These results constitute a motivation to conduct more in-depth studies, with the goal of better understanding the effect of variable atmospheric conditions on the attenuation of solar radiation after reflection by heliostats.

In this work, an extensive and detailed analysis of the aerosol transmittance is undertaken with MODTRAN for heliostat-to-receiver slant paths of varied lengths. Five aerosol models are used along with four atmospheric profiles and two different ground elevations. The combination of these aerosol models with the water-temperature-pressure profiles at each ground level generates a total of 40 different model atmospheres. The resulting large range of atmospheric conditions is analyzed in this study, with the underlying goal of developing a general simplified model.

2. Methodology

2.1 Slant atmospheric attenuation

The aerosol-induced irradiance attenuation A taking place along the mirror-to-receiver slant path is evaluated (in percent) by means of the following expression:

$$A = 100\,\frac{G_{bT0} - G_{bT}}{G_{bM}} \qquad \text{(eq. 1)}$$

where G_{bT0} is the reflected direct normal irradiance (DNI) reaching the receiver at the top of the tower assuming no aerosol, G_{bT} is the reflected DNI reaching the receiver but assuming the presence of aerosol, and G_{bM} is the DNI incident on the mirror (Fig. 1). The atmospheric conditions are assumed identical for both G_{bM} and G_{bT}. In this way, eq. (1) represents the percent fraction of energy loss due exclusively to aerosol extinction along the slant range considered. Additional extinction is expected, and would be caused primarily by water vapor (Gueymard et al., 2017; López et al., 2016).

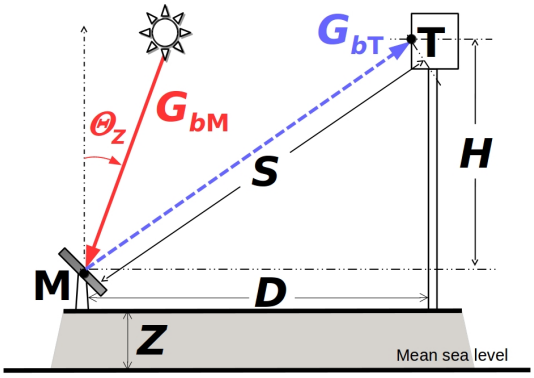

Fig. 1: Schematic description of a solar power tower plant, and nomenclature.

The irradiance incident on the mirror M, G_{bM}, and the irradiance reaching the tower receiver T reflected by the mirror (Fig. 1) may be obtained as:

$$G_{bM} = \int_{\lambda 1}^{\lambda 2} T_{\lambda M} G_{b\lambda 0}\,\mathrm{d}\lambda \qquad \text{(eq. 2)}$$

$$G_{bT} = \int_{\lambda 1}^{\lambda 2} \rho_{\lambda} T_{\lambda M-T} T_{\lambda M} G_{b\lambda 0}\,\mathrm{d}\lambda \qquad \text{(eq. 3)}$$

$$G_{bT0} = \int_{\lambda 1}^{\lambda 2} \rho_{\lambda} T_{\lambda M-T0} T_{\lambda M} G_{b\lambda 0}\,\mathrm{d}\lambda \qquad \text{(eq. 4)}$$

where $G_{b\lambda 0}$ is the extraterrestrial spectral irradiance, $T_{\lambda M}$ is the atmospheric spectral transmittance for the Sun-to-Mirror path (which depends on the abundance of various atmospheric constituents, and thus varies over time), $T_{\lambda M\text{-}T}$ is the spectral transmittance for the Mirror-to-Tower slant path taking into account the aerosol load, $T_{\lambda M\text{-}T0}$ is also the spectral transmittance for the Mirror-to-Tower slant path but considering no aerosols in the slant path, and ρ_λ is the mirror's spectral reflectance (set to 1 here for the sake of simplicity in this work). The integration limits are fixed to λ_1 = 0.28 μm and λ_2 = 10 μm. Following López et al. (2016), the solar zenith angle of the DNI incident on the mirror is varied incrementally from 0º to 89º, as shown in Table 1. Although TSP plants do not operate under large solar zenith angles, values higher than 80º are considered here in order to analyze the trend of transmission loss under these extreme limits.

Tab. 1: Values of the MODTRAN inputs used to obtain the simulated database.

Inputs to MODTRAN	Values
Θ_Z (degrees)	0, 10, 20, 30, 40, 50, 60, 70, 80, 85, 89
H (m)	100, 200, 250
D (km)	0.15, 0.5, 1, 2, 4
Z (km)	0, 1
Vis (km)	23, 50, 75
Aerosols Model	Rural, Maritime, Urban, Tropospheric, Desert
Atmospheric Model	MLW, MLS, Tropical, USSA

MODTRAN version 4v1r1 (Berk et al., 1989) is the radiative transfer code selected here for its remarkable capability of computing short-range transmittances. MODTRAN is the successor of LOWTRAN, which was used initially to demonstrate the impact of near-surface atmospheric constituents on the slant attenuation (Vittitoe and Biggs, 1978). MODTRAN is used parametrically to calculate each irradiance value in eqs. (2-4) for a number of specific atmospheric conditions. In particular, transmittances $T_{\lambda M\text{-}T}$ and $T_{\lambda M\text{-}T0}$ are obtained using MODTRAN's slant-path option, which evaluates the high-resolution spectral transmission between two points at finite distance—the mirror and the receiver, in the present case. MODTRAN considers the detailed effects of any vertical variation in atmospheric constituents, as well as the optical effects caused by atmospheric refraction and earth curvature..

2.2 Visibility and optical characteristics of aerosols

MODTRAN evaluates the radiative impact of aerosols as a function of their abundance. The latter is reported in terms of "visibility", whose definition needs to be clarified here. In meteorological terms, visibility is an old *subjective* estimation technique based on a human observer's evaluation of the maximum distance at which distant objects can be distinguished against a contrasting background, usually the sky. Modern instruments, like visibilimeters or transmissometers, now provide an *objective* evaluation of visibility, which is referred to as "meteorological optical range" (MOR), according to Koschmieder's law (Koschmieder, 1925):

$$MOR = \frac{\ln\left(1/\varepsilon\right)}{\sigma} \qquad \text{(eq. 5)}$$

where σ is the air extinction coefficient at 550 nm and ε is the threshold contrast between an object and the background. According to the World Meteorological Organization (WMO, 2014), ε must be set to 0.05 to obtain MOR. Another definition, referred to as "meteorological range" (MR) in MODTRAN, uses a more optimistic threshold contrast ε = 0.02:

$$MR = \frac{\ln\left(1/0.02\right)}{\sigma} \qquad \text{(eq. 6)}$$

It is straightforward to perform the conversion between these two definitions: MR = 1.306 MOR. The relationship given by eq. (5) or (6) may be deceptively simple, however, since its derivation depends on a number of serious assumptions (Middleton, 1952). Even though MODTRAN and its predecessor, LOWTRAN, use the term "visibility" to describe the aerosol input, what is actually meant is MR, which is highly confusing, since it is different from MOR. Kneizys et al (1980) acknowledged the difference between MR and observer (subjective) visibility, V_{obs}, and indicated that MR ≈ (1.3 ± 0.3) V_{obs}. (The coefficient 1.3 simply represents the ratio MR/MOR = ln(1/0.02)/ln(1/0.05).) Hence, MOR is just a technical term for what was previously known as "observer visibility", or V_{obs}. In what follows, the abbreviation VIS is used to conform to MODTRAN's usage, even though the intended variable name is MR.

One key issue of using VIS to describe the optical impact of aerosols is the limited number of monitoring sites, mostly at airports. Hence, access to actual local data is difficult in practice. In comparison, there are many more sources of data that provide the aerosol optical depth (AOD), based on ground measurements with sunphotometers, chemical transport models (and derived reanalysis models), or space borne remote-sensed observations. Additionally, visibilimeters installed at airports have a very limited range, typically 20 km (Gueymard, 2012), which is not enough to provide the precise inputs needed here. A relationship between VIS and AOD is thus desirable, so that VIS can be estimated from AOD observations, or vice versa. Experimental studies have shown that the two variables are only weakly correlated in practice, due to a number of difficulties (Wilson et al., 2015). For the present study, what is important is the theoretical correspondence between VIS and AOD, as specifically applicable to MODTRAN. This desired relationship is built in SMARTS (Gueymard, 2001) to allow the conversion of VIS to AOD or vice versa. Table 2 provides the needed information to allow comparisons between the results presented here (based on VIS) and those provided in other studies that are rather based on AOD (Sengupta et al., 2012).

Tab. 2: Approximate equivalence between Meteorological Range (as used in MODTRAN), Visibility, and Aerosol Optical Depth at 550 nm, based on SMARTS simulations.

Meteorological Range (km)	Observer/Subjective Visibility (km)	AOD at 550 nm
5	3.8	1.1730
10	7.7	0.6667
15	11.5	0.4744
20	15.4	0.3686
23	17.7	0.3251
25	19.2	0.3014
50	38.5	0.1596
75	57.7	0.1126
100	76.9	0.0901
150	115.4	0.0667
200	153.8	0.0549

Various aerosol loads are considered in this study by means of three surface visibility values: 23, 50 and 75 km (higher visibilities correspond to lower aerosol optical depths, as shown in Table 2). Various aerosol models are available in MODTRAN, and can be selected in order to analyze the effect of the optical properties of each possible aerosol type on transmission losses. Five common aerosol models are selected here: rural, maritime, urban, tropospheric, and desert (Tab. 1). The desert aerosol model is an important aerosol type since it is representative of arid and semiarid regions, which are favorite emplacements for TSP plants due to the high DNI resource there. The desert aerosol model is dependent on wind speed, leading to the expectation that the slant-path attenuation will increase with wind speed. This is mainly due to the hematite contained in sand particles, which leads to selective absorption at visible wavelengths, becoming more pronounced when it is entrained as wind speed increases (Longtin et al., 1988). In this first analysis, wind speed is fixed to 10 m s^{-1}, corresponding to the reference value given in MODTRAN.

2.3 Other variables

Since the concentration and mixture of aerosol particles have variable vertical profiles, the potential influence of ground elevation on transmission losses is explored by considering two site elevations, Z = 0 km and 1 km above mean sea level. For elevated sites (e.g., Z = 1 km), MODTRAN´s modeling is more elaborate than at sea

level. The aerosol densities below 6 km are subjected to vertical compression, in such a way that the aerosol sources are moved up to that altitude. Hence, the energy loss computation may be performed using visibility observations at the elevated site, which eliminates the need for additional calculation (scaling between sea level and the actual site elevation). In other words, MODTRAN transparently takes into account the fact that the aerosol concentration near the surface at an elevated site is normally larger than in the free atmosphere at the same altitude.

In addition to the above variables, which are explicitly related to the aerosol effect, the impact of different atmospheric water-temperature-pressure profiles on the transmission losses by aerosols is also analyzed by means of four built-in standard atmosphere models: Mid-Latitude Winter (MLW), Mid-Latitude Summer (MLS), Tropical, and U.S. Standard Atmosphere (USSA). The spectral distribution of DNI both at the mirror and at the receiver is modified according to the atmosphere model. Consequently, the transmission loss by aerosols can also be expected to differ. All the gaseous concentrations (such as water vapor) are set to the reference values imposed by the selected atmosphere model.

Finally, different slant ranges are considered between mirror and receiver. The geometries selected here attempt to mimic the typical configurations encountered in current or future TSP plants. Three tower heights, H, are used (100, 200 and 250 m), as well as five values for the horizontal mirror-to-tower distance D (0.15, 0.5, 1, 2 and 3 km). The resulting combinations of H and D represent a large range of possible geometries, which is needed to generalize the results.

3. Results

3.1 Effect of zenith angle

Figure 2 shows the transmission losses, A, or "energy losses" due to aerosols alone, as a fraction of G_{bM} for a set of atmospheric conditions: eleven zenith angles between 0º and 89°, three slant ranges, S, corresponding to the combination of a single tower height (H = 100 m) with three mirror-to-tower horizontal distances (D = 0.15, 1, and 4 km), ground at sea level (Z = 0 m), and three visibilities (23, 50, and 75 km). All five aerosols models are used here, combined with the MLS atmosphere.

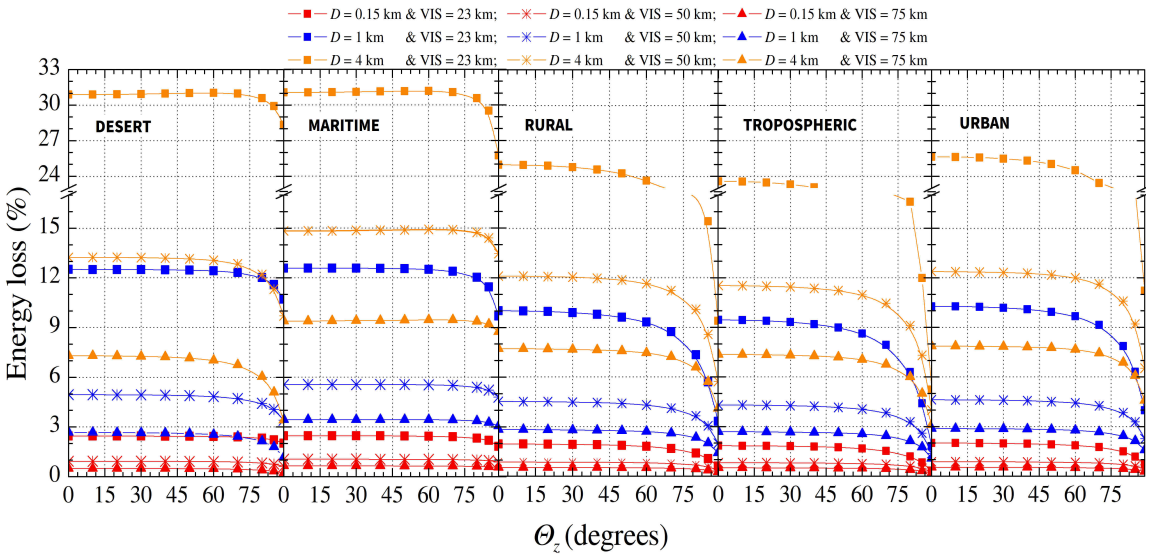

Fig 2. Energy losses in the mirror-to-receiver slant path versus zenith angle for five different types of aerosol, using the MLS Atmosphere, three visibilities (23, 50 and 75 km), a tower height of 100 m, three horizontal mirror-to-tower distance (D = 0.15, 1 and 4 km) and a site at sea level (Z = 0 m).

For short distances (D = 0.15 km), the energy losses are almost constant for any visibility and any aerosol model. The impact of zenith angle is also found negligible over the normal operation range of TSP plants. In contrast, when slant range increases (using D = 1 and 4 km), the energy losses corresponding to the rural, urban and tropospheric aerosol models show a higher dependence with zenith angle, and get stronger when D increases. When the sun rises and Θ_Z decreases from 75º to 30º, energy losses increase by 2% in the case of rural

and urban aerosols, and even more for tropospheric aerosols. This relationship with zenith angle is also observed for the energy losses that are specifically due to water vapor (López et al., 2016). The type of aerosol mixture is important here, since desert or maritime aerosols do not produce this marked zenith angle dependence, at least for $\Theta_Z < 80º$. The results shown in Fig. 2 are representative of those corresponding to the other tower heights, horizontal mirror-to-tower distances, ground elevations and atmospheric profiles.

3.2 Effect of atmosphere model

Similar to Fig. 2, Fig. 3 shows the calculated energy losses as a function of zenith angle for a slant range corresponding to a tower height H = 100 m, a mirror-to-tower horizontal distance D = 1 km, ground at sea level (Z = 0 m), and two different visibilities, 23 and 75 km. The five aerosols models and all four atmosphere models are used here to evaluate their combined effects.

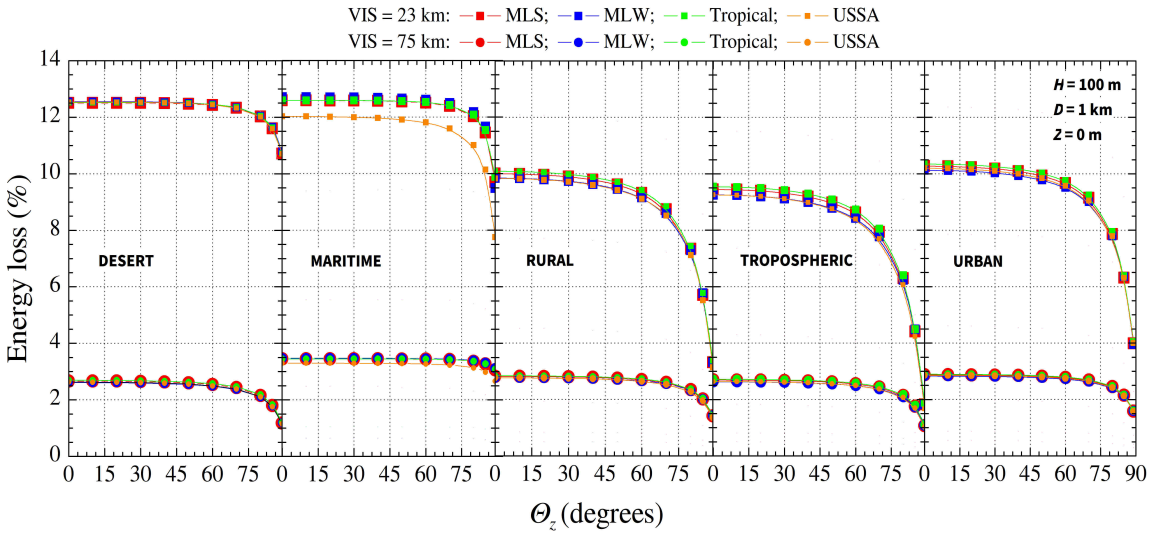

Fig 3. Energy losses in the mirror-to-receiver slant path versus zenith angle for five different types of aerosol and four atmosphere models, using two visibilities (23 and 75 km), a tower height of 100 m, a horizontal heliostat-to-tower distance D = 1 km, and a site at sea level.

In general, it is found that the atmosphere model has little impact, if not negligible. With the desert aerosol model, for instance, all four atmosphere models provide the same energy loss for each of the two visibilities (23 km and 75 km), with maximum energy losses of about 13% and 3%, respectively. This means that the desert aerosol model appears insensitive to changes in meteorological conditions such as temperature, pressure, relative humidity, or water vapor content. This tendency is also observed with the remaining four aerosol models when used under very clear conditions (VIS = 75 km). Moreover, under such ideal conditions, all types of aerosol mixtures yield a similar energy loss of ≈3%, except for the maritime aerosol (≈3.5%). When visibility reduces to 23 km, the energy losses exhibit a weak dependence on the type of atmosphere model, with differences lower than 0.5%. The only exception is when the USSA atmospheric model is used along with the maritime aerosol, which leads to energy losses lower than 1% compared to what is obtained with the MLS, MLW or Tropical atmospheres. This is likely caused by the high sensitivity of the optical properties of maritime aerosols to variations in relative humidity. As a matter of fact, the aerosol mixtures of oceanic origin have significantly different properties compared to continental aerosol types, in particular (Shettle and Fenn, 1979). In the lower atmosphere, the MLS, MLW and Tropical atmospheres have vertical profiles of relative humidity that are similar between each other, but significantly different from the USSA model.

3.3 Effect of ground elevation

Site elevation has been identified as a critical factor by Pitman and Vant Hull (1982), and thus deserves attention. Its effect is analyzed here by evaluating the energy losses for two surface elevations (Z = 0 and 1 km), while parametrically varying the sun's zenith angle and using the MLS atmosphere for various conditions: H = 100 m, D = 1 km, the five aerosol models, and two visibilities. The results appear in Fig. 4a for VIS = 23 km and Fig. 4b for VIS = 75 km. It is observed that the elevation effect seems negligible in all cases, since the energy losses are almost identical for any input configuration at a specified Z. This is contrary to the Pitman and

Vant-Hull (1982) conclusions, which was not expected. A likely explanation for this discrepancy is that MODTRAN (used here) and LOWTRAN (used by Pitman and Vant Hull, among others) differ on how they consider visibility at an elevated site. This is directly related to the vertical aerosol scaling that is performed transparently by MODTRAN (but not in LOWTRAN), as mentioned above. It is also possible that the assumptions and results provided here, which are relative to aerosol-induced losses only, are not exactly compatible with those of Pitman and Vant Hull. This will require further scrutiny.

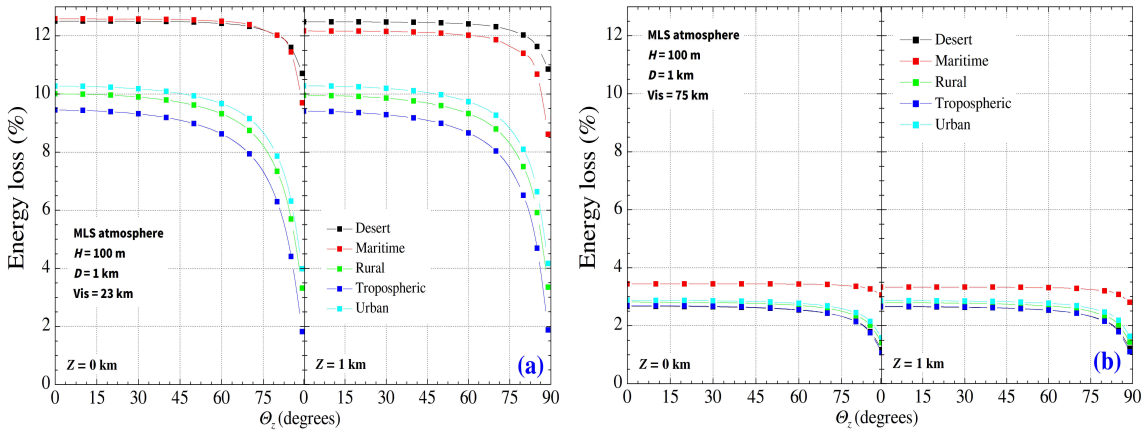

Fig 4. Energy losses versus zenith angle for five types of aerosol and two visibilities: (a) VIS = 23 km, and (b) VIS = 75 km. The MLS atmosphere, a tower height of 100 m, a horizontal mirror-to-tower distance *D* = 1 km, and two ground altitudes (*Z* = 0 and 1 km) are selected in both cases.

3.4 Effect of slant path range

The last parameters to be analyzed are those determining the length of the slant path *S* followed by the reflected sun rays from the mirror up to the receiver at the top of the tower: the horizontal mirror-to-tower distance *D* and the tower height *H*. Figure 5 displays the energy loss for a fixed zenith angle (Θ_z = 30º) and various combinations of *D* and *H*, per the values listed in Table 1. Under very clear conditions, corresponding to VIS = 75 km, the energy loss is not sensitive to variations in tower height, even though the aerosol concentration normally decreases with elevation in the free atmosphere. It is possible that this lack of sensitivity reflects the crude vertical resolution (1 km) of aerosol and atmosphere models in MODTRAN.

Desert, rural, tropospheric and urban aerosol determine similar energy losses, ranging from < 1% for *D* = 0.15 km, up to 7% for *D* = 4 km. The attenuation due to maritime aerosols is slightly higher, reaching a maximum of 9%. When a lower visibility (23 km) is considered, the influence of *H* on *A* is weak for large distances (*D* > 2 km), and becomes imperceptible for short distances (*D* < 2 km). Only the attenuation due to maritime aerosols shows any dependence on tower height. The results for the other atmospheres are similar to this.

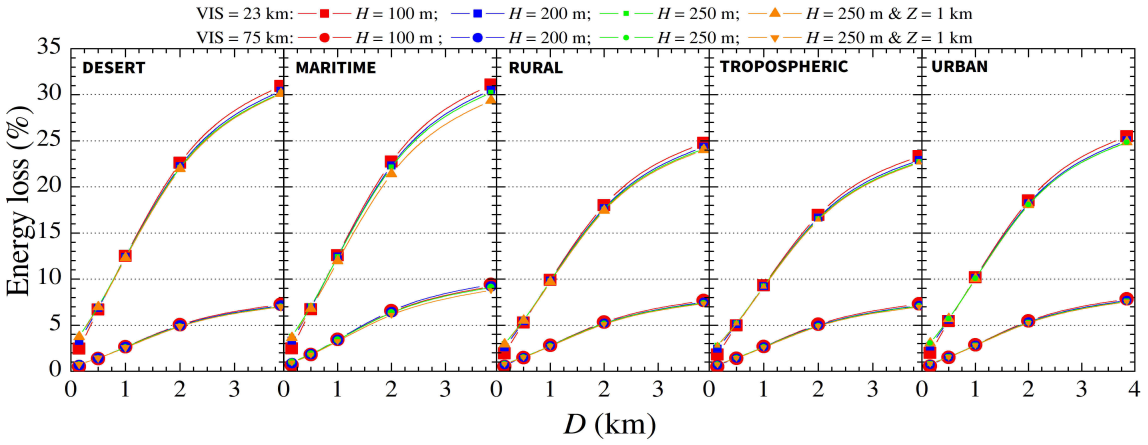

Fig 5. Energy losses vs. horizontal mirror-to-tower distance for five different types of aerosol. All cases use the MLS atmosphere, two visibilities (23 and 75 km) and three tower heights (*H* = 100, 200 and 250 m). In addition, the red, blue and green lines correspond to *Z* = 0 km, whereas the orange line is for *Z* = 1 km.

3.5 Generalized results

The results provided above show how energy losses depend on a number of variables. Some of these variables have more impact than others. Because of the intricacies of all the implied relationships, it is desirable to derive a simplified, generalized model. Results for the desert and maritime aerosols are similar, but differ from those obtained with the other three aerosol models. A simplification thus consists in considering only two distinct groups of possible aerosols: Either desert/maritime or rural/urban/tropospheric. In each group, the energy losses do not vary much with aerosol type, so that an aerosol-independent average can be used for simplification. Moreover, since tower height, atmosphere model, surface elevation and zenith angle have no significant effects, the only remaining critical factors are VIS and *D*. Plots providing the energy loss *A* as a function of VIS and *D* for each aerosol group appear in Fig. 6. As could be expected, *A* is a strong function of both VIS and *D*. *A* is also affected by the aerosol group, but to a lower extent—particularly for high visibilities. In theory, these plots can also be used to rather relate *A* to AOD and *D*, using the data in Tab. 2. As noted above, however, the relationship between VIS and AOD is not an exact one under real conditions. Hence, additional studies would be needed to better establish the relationship between *A* and on-site AOD observations, for instance.

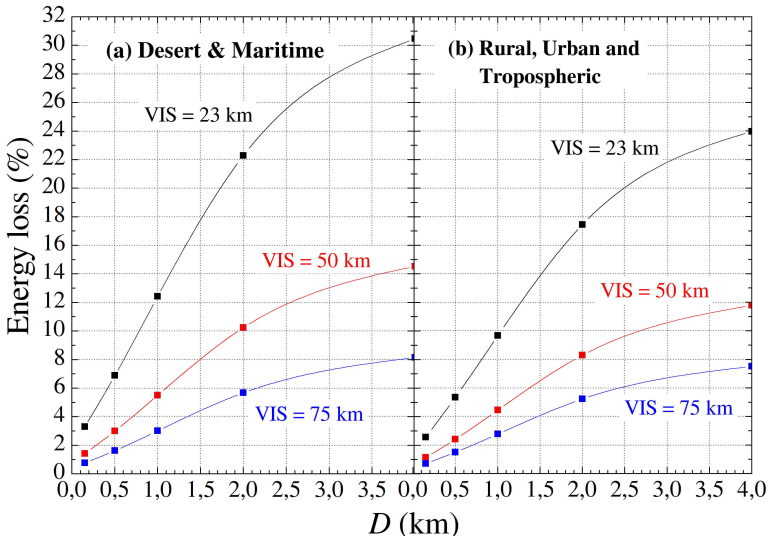

Fig. 6. Generalized results relating the energy lost between a mirror and the tower receiver to VIS and horizontal distance *D* for two distinct groups of aerosols.

4. Conclusions

For Tower Solar Plants (TSP), the energy losses for the mirror-to-tower slant path caused by the presence of aerosols near the ground have been analyzed as a fraction of the DNI incident on the mirror. Many different configurations of possible TSP geometries and atmospheric conditions were employed to generate the transmission losses, using the MODTRAN spectral atmospheric code with its slant-path option. A first result obtained here is that the energy loss does not appreciably depend on the specific atmosphere model that can be selected in MODTRAN (e.g., mid-latitude winter, mid-latitude summer, tropical or USSA). This leads to an important simplification, since the energy loss caused by aerosols can be properly calculated for any site using only one atmospheric profile. Similarly, the energy loss is virtually independent from the sun's zenith angle (up to ≈75°), and does neither depend on ground elevation, nor on the TSP's tower height. The main atmospheric variable driving the energy loss caused by aerosols is visibility (or more precisely, "meteorological range", per MODTRAN's definition). Selecting various types of aerosol (rural, urban, tropospheric, maritime, or desert) leads to different energy losses and different dependences on the sun's zenith angle. However, the five aerosol models may be reduced to only two categories: (i) 'optically thin aerosols', consisting of the rural, urban and tropospheric aerosols, which yield maximum energy losses lower than 25% for a 23-km visibility and 4-km horizontal distance; and (ii) 'optically thick aerosols' composed of the desert and maritime aerosols, generating maximum energy losses of 30% for the same visibility and distance.

Taking some possible simplifications into account, all results can be synthesized into two plots (one for each aerosol group) that provide the aerosol-induced energy losses at any site as a function of visibility and horizontal mirror-to-tower distance. A theoretical correspondence between visibility, as defined here, and aerosol optical depth is also provided, in case visibility measurements are not available. Finally, the present results will allow the development of future parameterizations of the transmission losses, based on only a limited number of essential variables. In addition, the proposed results can be used as benchmark values for assessing the performance of other models of the literature, such as those used in various CSP design codes.

5. Acknowledgments

The authors are grateful for the financial support provided by the Spanish Project "PRESOL" ENE2014-59454-C3-2-R, which is funded by the Ministerio de Economía y Competitividad and co-financed by the European Regional Development Fund (FEDER).

6. References

Berk, A., Bernstein, L.S., Robertson, D.C., 1989. MODTRAN: A Moderate Resolution Model forLOWTRAN7. Report GL-TR-89-0122, Air Force Geophysical Laboratory, Hanscom, MA.

Gueymard, C.A., 2001. Parameterized Transmittance Model for Direct Beam and Circumsolar Spectral Irradiance. Solar Energy 71, 325-346.

Gueymard, C.A., 2012. Visibility, aerosol conditions, and irradiance attenuation close to the ground. Solar Energy 86, 1667-1668.

Gueymard, C.A., López, G., Rapp-Arrarás, I., 2017. Atmospheric transmission loss in mirror-to-tower slant ranges due to water vapor. AIP Conference Proceedings, 1850, 140010; doi: 10.1063/1.4984518

Hanrieder, N., Sengupta, M., Xie, Y., Wilbert, S., Pitz-Paal, R., 2016. Modeling beam attenuation in solar tower plants using common DNI measurements. Solar Energy, 1529, 244–255.

Hanrieder, N., Wilbert, S. Mancera-Guevara, D., Buck,R., Giuliano, S., Pitz-Paal, R., 2017. Atmospheric extinction in solar tower plants – A review. Solar Energy, 152, 193-207.

Kneizys, F.X., Shettle, E.P., Gallery, W.O., Chetwynd, J.H., Abreu, L.W., Selby, J.E.A., Fenn, R.W., McClatchey, R.A., 1980. Atmospheric transmittance/radiance: Computer code LOWTRAN 5. Report AFGL-TR-80-067, Air Force Geophysics Lab., Hanscom AFB, MA.

Koschmieder, H., 1925. Theorie der horizontalen Sichtweite, Keim & Nemnich.

Longtin, D. R., Shettle, E. P., Hummel, J. R., Pryce, J.D., 1988. A Wind Dependent Desert Aerosol Model: RadiativeProperties, AFGL-TR-88-0112, Air Force Geophysics Laboratory, Hanscom AFB, MA.

López, G., Gueymard, C.A., Bosch, J.L., Rapp-Arrarás, I., Alonso-Montesinos, J., Ballestrín, J., Polo, J., Barbero, J., Pulido-Calvo, I., 2016. Modelling water vapor impact on the solar energy reaching the receiver of a solar tower plant by means of artificial neural networks. . Proc. 11th EuroSun Conference, Palma de Mallorca, Spain, International Solar Energy Soc.

López, G., Bosch, J.L., Pulido-Calvo, I., Gueymard, C.A., 2017. Visibility Estimates from Atmospheric and Radiometric Variables Using Artificial Neural Networks. Proc. Air Pollution XXV Conf., WIT Transactions on Ecology and The Environment, vol 211, 129-136; doi:10.2495/AIR170131.

Middleton, W.E.K., 1952. Vision through the atmosphere. Univ. Toronto Press.

Pitman, C.L., Vant-Hull, L.L., 1982. Atmospheric transmittance model for a solar beam propagating between a heliostat and a receiver. ASES Progress in Solar Energy, 1247–1251.

Sengupta, M., Wagner, M., 2012.Atmospheric attenuation in central receiver systems from DNI measurements. Proc. Solar 2012 Conf., Denver, CO, American Solar Energy Soc.

Shettle, E.P., Fenn, R.W., 1979. Models for the aerosols of the lower atmosphere and the effects of humidity variations on their optical properties. Report AFGL-TR-79-0214, Air Force Geophysics Lab., Hanscom AFB.

Vittitoe, C., Biggs, F, 1978. Terrestrial propagation loss. Proc. American Section of ISES annual meeting, Denver, CO, 664–668.

Wilson, R.T., Milton, E.J., Nield, J.M., 2015. Are visibility-derived AOT estimates suitable for parameterizing satellite data atmospheric correction algorithms? International Journal of Remote Sensing 36, 1675-1688, 10.1080/01431161.2015.1023558.

WMO, 2014. Measurement of Visibility, in WMO No-8 2014, Guide to Meteorological Instruments and Methods of Observation (CIMO guide). Geneva, Switzerland. https://library.wmo.int/opac/doc_num.php?explnum_id=3121.